Journal of Chromatography, 517 (1990) 423–433
Elsevier Science Publishers B.V., Amsterdam

CHROMSYMP. 1949

Evaluation of pinched inlet channel for stopless flow injection in steric field-flow fractionation

MYEONG HEE MOON, MARCUS N. MYERS* and J. CALVIN GIDDINGS
Field-Flow Fractionation Research Center, Department of Chemistry, University of Utah, Salt Lake City, UT 84112 (U.S.A.)

ABSTRACT

In this article the concept of utilizing a pinched inlet channel for field-flow fractionation (FFF), in which the channel thickness is reduced over a substantial inlet segment to reduce relaxation effects and avoid stopflow, is evaluated for steric FFF using one conventional channel and two pinched inlet channels. It is shown that with the proper adjustment of flow-rate, the stopflow process in FFF can be completely avoided, thus bypassing the flow interruption associated with stopflow and reducing separation time. The maximum flow-rate that can be used for stopless flow operation without incurring zone distortion is shown to agree reasonably well with simple theory; slight departures from theory are attributed to the existence of reduced transport rates of large particles through thin channel structures.

INTRODUCTION

In a previous paper it was suggested that the relaxation process in field-flow fractionation (FFF) can be hastened by reducing the thickness of the FFF channel at the inlet end[1]. The use of such a modified channel structure, designated by the term "pinched inlet channel", has the potential of reducing separation time in FFF, reducing the adhesion of sample material to the channel walls and, in some instances, simplifying the FFF procedure. The object of this work is to achieve the first implementation of pinched inlet FFF. The system chosen for this study is a steric FFF channel utilizing a gravitational driving force.

FFF is generally carried out by using a stopflow procedure[2]. Here, following sample introduction, the channel flow is stopped for a time of sufficient duration to permit the sample material, under the influence of the driving force, to accumulate in the vicinity of one of the channel walls. After accumulation, the flow is restarted and the separation process is carried out. The purpose of the stopflow procedure is to reduce the band broadening associated with the accumulation or "relaxation" process[2]. However, the stopflow procedure has two or three negative side-effects. First, stopflow lengthens the time required for completion of the run, sometimes by

0021-9673/90/$03.50

a substantial amount[3]. Second, stopflow requires the interruption of flow, which is not only experimentally awkward but is capable of causing baseline perturbations due to the pressure transients associated with the flow changes. Third, the static conditions encountered in stopflow are conducive to the adhesion of sample particles to the channel wall, which may cause sample loss. For all these reasons it would be desirable to eliminate the stopflow procedure providing excessive band broadening could somehow be avoided.

By reducing the channel thickness at the inlet end, the relaxation time, equal to the time required for a given component to be transported across the thickness of the channel, is reduced. Therefore the stopflow time t_{sf} can be correspondingly decreased. Even if the channel flow is maintained and stopflow avoided, the incremental band broadening associated with relaxation in such a system is greatly reduced relative to its magnitude in conventional FFF channels of uniform thickness. Specifically, theory indicates that the increment in the variance in elution time of a component carried at a given flow-rate in an FFF channel increases with the fourth power of channel thickness w providing the relaxation process is confined to a segment of constant thickness[1]. In order to take full advantage of this strong dependence on w, it is necessary to reduce the channel thickness at the inlet end. Moreover, in order to realize full relaxation within the confines of this pinched inlet or relaxation segment without stopping the flow, the pinched segment must extend a substantial distance into the channel. It is very likely that pinched inlet segments that occupy approximately 50% of the channel length will prove highly practical in the implementation of the pinched inlet concept. In the present study, 40% of the channel length is utilized for the relaxation segment.

While the pinched inlet concept will be most ideally realized by using a constant and uninterrupted flow throughout the FFF process, there will be occasions in which the relaxation time is so large that full relaxation cannot be achieved in the pinched inlet section at normal channel flow-rates. In that instance, the channel flow-rate can be reduced to a value that will allow for the full relaxation of the slowest component in the pinched sector. Following the relaxation of all components, normal flow is resumed. With this *slow flow injection* procedure, there is still an abrupt flow change (although the magnitude of the change is reduced), but one would still have the advantage of a reduced analysis time associated with the reduced relaxation time. Alternatively, one could revert to the normal stopflow procedure while using a pinched inlet, again realizing the advantage of a reduced relaxation time and faster analysis.

The pinched inlet concept appears to be applicable to all of the normal operating modes of FFF, including sedimentation FFF, thermal FFF, flow FFF, and electrical FFF[1]. It would appear to be particularly advantageous for programmed field operation. It should also be applicable to the characterization of larger particles ($\geqslant 1$ μm diameter) by steric FFF. The simplicity of a steric FFF channel system designed to utilize the earth's gravity as a driving force is an important factor in choosing steric FFF for the initial evaluation of the pinched inlet concept.

THEORETICAL

The essential equations governing the behavior of a pinched inlet system used in the steric FFF mode are summarized below. We start with the central parameter, the relaxation time τ, given by the following expression

$$\tau = \frac{w}{U} \tag{1}$$

where w is the channel thickness and U is the field-induced velocity of the particle driven across the channel. Because of the finite relaxation time, the particle band broadens out into a bimodal distribution along the flow coordinate[4]. The distance h_0 between band extremities is given by

$$h_0 = \frac{\dot{V}}{bU} \tag{2}$$

where $\dot{V}$ is the volumetric flow-rate through the channel and b is the channel breadth. We note that this expression for band width is independent of channel thickness w.

Because of relaxational band broadening represented by h_0, the peak emerging from the FFF system is incrementally broadened in time units. The time-based variance of the peak induced by relaxation is given by[1]

$$\sigma_t^2 = \frac{17}{140}\frac{\tau^2}{R^2} \tag{3}$$

where R is the retention ratio of the particle band in the pinched segment of the channel. With the help of eqn. 1 this expression assumes the form

$$\sigma_t^2 = \frac{17}{140}\frac{w^2}{U^2R^2} \tag{4}$$

This equation is generally valid for most operating forms of FFF. For steric FFF, we substitute the applicable expression for R (ref. 5)

$$R = \frac{3\gamma d}{w} \tag{5}$$

which converts eqn. 4 into the previously derived expression for steric FFF[1]

$$\sigma_t^2 = 0.0135\frac{w^4}{\gamma^2 d^2 U^2} \tag{6}$$

Under the influence of a sedimentation field of acceleration G, the settling velocity for a particle obeying Stokes equation is given by[6]

$$U = \frac{d^2 \Delta\rho G}{18\eta} \tag{7}$$

where $\Delta\rho$ is the density difference between the particle and the liquid carrier and η is the viscosity. With the help of this expression, eqns. 1, 2 and 6 become

$$\tau = \frac{18\eta w}{d^2 \Delta \rho G} \tag{8}$$

$$h_0 = \frac{18\eta \dot{V}}{d^2 \Delta \rho G b} \tag{9}$$

$$\sigma_t^2 = \frac{4.37\, w^4 \eta^2}{\gamma^2 d^6 \Delta \rho^2 G^2} \tag{10}$$

The last equation shows that the time-based variance originating in relaxation is proportional to the fourth power of channel thickness w and inversely proportional to the sixth power of particle diameter d. We note that these dependencies are slightly modified by the correction term γ, which will exhibit a slight dependence on both w and d (ref. 5).

Plate height

The apparent (or measured) plate height in a chromatographic or FFF elution system is given by

$$\hat{H} = L \frac{\sigma_t^2}{t_R^2} \tag{11}$$

where σ_t^2 is the observed variance in time units, t_R is the retention time, and L is the length of the column or channel.

For a segmented system such as the pinched inlet channel, the apparent plate height is related to the plate heights (H_1 and H_2) of the two segments by[7]

$$\hat{H} = \frac{\dfrac{H_1 L_1}{R_1^2 < v_1 >^2 L} + \dfrac{H_2 L_2}{R_2^2 < v_2 >^2 L}}{\left[\dfrac{L_1}{R_1 < v_1 > L} + \dfrac{L_2}{R_2 < v_2 > L}\right]^2} \tag{12}$$

where the lengths, retention ratios, and mean cross-sectional velocities in the two successive segments are L_1 and L_2, R_1 and R_2, and $< v_1 >$ and $< v_2 >$, respectively. If the mean velocity ($R_1 < v_1 >$) of the particle band in segment 1 (the pinched segment) is M times larger than its velocity ($R_2 < v_2 >$) in segment 2, eqn. 12 becomes[7]

$$\hat{H} = \frac{H_1 \dfrac{L_1}{L} + M^2 H_2 \dfrac{L_2}{L}}{\left(\dfrac{L_1}{L} + M \dfrac{L_2}{L}\right)^2} \tag{13}$$

For both channels used here, $L_1/L = 0.4$ and $L_2/L = 0.6$. With these values $\hat{H}$ reduces to

$$\hat{H} = \frac{0.4H_1 + 0.6M^2H_2}{(0.4 + 0.6M)^2} \tag{14}$$

Because $<v>$ and R (see eqn. 5) are both inversely proportional to channel thickness w (a conclusion valid for normal as well as steric FFF), M can be written as

$$M = \frac{R_1\langle v_1\rangle}{R_2\langle v_2\rangle} = \left(\frac{w_2}{w_1}\right)^2 \tag{15}$$

Thus for channel I, for which $M = 4$, $\hat{H}$ is

$$\hat{H} = 0.0510H_1 + 1.2245H_2 \tag{16}$$

For channel II, for which $M = 100/9$, we get

$$\hat{H} = 0.0080H_1 + 1.4833H_2 \tag{17}$$

These equations show (by way of specific examples) that excessive band broadening (large H_1) due to relaxation effects is largely cancelled out by the small weighting factors associated with the rapid transit through the constricted relaxation segment. Furthermore, it can be shown that H_1 due to relaxation approaches a maximum of 0.1214 L_1 for particles whose relaxation distance $h_0 \rightarrow L_1$. (The justification for the weighting factor for H_2 exceeding unity can be found in ref. 7.)

Plate height H_1 consists of contributions both from relaxation (which becomes the dominant term when h_0 is a significant fraction of L_1) and from normal band broadening processes. To a first approximation, H_1 can be expressed as the sum of the two contributions

$$H_1 = H_1(\text{relaxation}) + H_1(\text{stop flow}) \tag{18}$$

where H_1(relaxation) is based on the variance obtained from eqns. 3, 4, 6, or 10 and H_1(stop flow) is the plate height observed under stopflow conditions in which band broadening due to relaxation is eliminated.

EXPERIMENTAL

For the purposes of comparison two channel geometries were used, one with and one without the pinched inlet configuration. The channel volumes were cut out of thin plastic spacers and sandwiched between glass plates, then clamped together between Lucite bars. This general structure, described in an earlier publication[8], has been found suitable for steric FFF using gravity as the driving force.

A Teflon spacer of 254 μm thickness was used for the uniform channel (lacking a pinched inlet). The channel, cut from the spacer, has a tip-to-tip length L of 38.4 cm and a breadth b of 2 cm. The void volume, measured as the elution volume of an unretained sodium benzoate peak, is 1.84 ml.

Two pinched inlet channels were constructed. Both utilized two sheets of Mylar

in their construction, one with the full channel length removed and the other cut in such a way that a "blocking element" was left in place. The blocking element is a strip of material that occupies the inlet end of the channel in order to reduce its thickness and thus realize the pinched inlet geometry[1]. The construction of the systems is illustrated in Fig. 1. The combined thickness of the two films is 254 μm in both cases, the same as the thickness of the uniform channel. For pinched inlet channel I, the two thicknesses are both 127 μm. For channel II, the film with the blocking element is 178 μm thick and the film from which the pinched inlet is cut is 76 μm thick. The length (38.4 cm) and breadth (2 cm) of the pinched inlet channel systems are identical to those used for the uniform channel. The length L_1 of the blocking element, measured from the channel tip to the blocking edge, is 15.4 cm in both cases, 40% of the total length. The void volumes, also measured with a non-retained peak, are 1.52 ml for channel I and 1.41 ml for channel II.

The samples used in this study were polystyrene latex beads (Duke Scientific, Palo Alto, CA, U.S.A.) with mean diameters of 15 and 20 μm. The carrier liquid was doubly distilled water with 0.01% FL-70 detergent (Fisher Scientific, Fairlawn, NJ, U.S.A.) and 0.02% sodium azide used as a bacteriocide. All runs were carried out at room temperature, 293 $\pm$ 1 K. From 15 to 20 μl of the sample suspension (containing $2 \cdot 10^4$–$3 \cdot 10^4$ particles) was injected into the channel through a septum by means of a microsyringe.

For the stopflow method the sample was slowly carried to the head of the channel with a Gilson (Madison, WI, U.S.A.) Minipuls 2 pump. The flow was then completely stopped for a period adequate to allow the particles to relax to the accumulation wall. The relaxation time was calculated from the Stokes–Einstein equation. Following relaxation, flow was resumed.

In the case of stopless flow injection, the sample was introduced by syringe directly into the carrier stream. The flow of the latter was held constant, without change or interruption.

The eluted sample was monitored by a Model 106 UV detector, from Linear

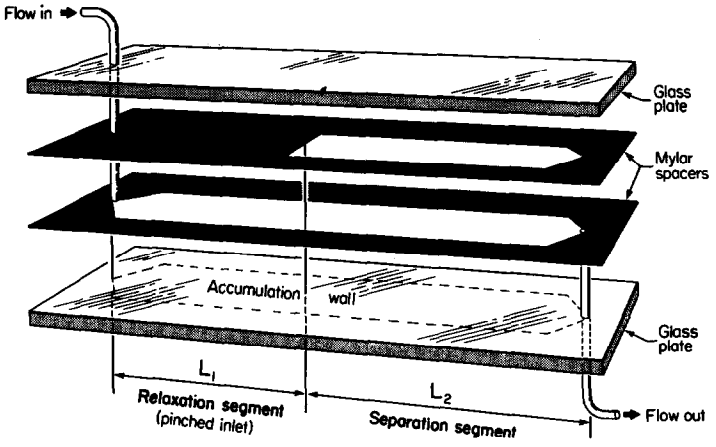

Fig. 1. Layers assembled to form pinched channel system.

Instrument (Reno, NV, U.S.A.) at a wavelength of 229 nm. A strip chart recorder from Houston Instrument (Austin, TX, U.S.A.) was used to record the emerging peaks.

RESULTS AND DISCUSSION

Fig. 2 shows three different elution profiles for the 15-μm polystyrene latex spheres run at the same flow-rate, 0.73 ml/min, equivalent to a linear flow velocity of 0.24 cm/s in the separation segment of the channel where the channel thickness (254 μm) is greatest. Fig. 2a shows the concentration profile of the particles emerging from the reference (uniform or non-pinched) channel after application of the stopflow procedure. For this case the stopflow time was 42 s, equal to the calculated relaxation time of the particles across the full channel thickness (254 μm). Fig. 2b shows the results of a run identical in all respects to that of Fig. 2a except that the stopless flow procedure was used to bypass the flow interruption of stopflow. The emerging peak in this case shows a substantial loss of sharpness as expected for stopless flow operation. (For smaller particles with longer relaxation times than that of the 15-μm particle, the stopless flow profile would be much broader and would have a bimodal shape.) We also observe that the trailing edge of the peaks in Fig. 2a and b nearly coincide in their positions; the leading edge of the Fig. 2b profile, however, appears considerably earlier than that for the Fig. 2a peak as a consequence of the accelerated elution of those particles starting the run near the top wall of the channel where relaxation effects are maximal.

Fig. 2c shows the profile of the 15-μm beads emerging from pinched inlet channel system I after stopless flow injection. We observe that the excessive band broadening illustrated by Fig. 2b has been eliminated through the use of the pinched inlet channel. The band width is comparable to that in Fig. 2a for normal stopflow operation. More

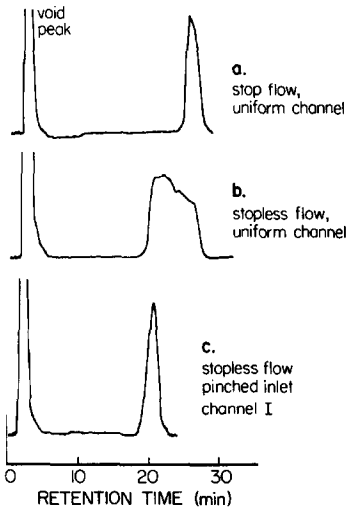

Fig. 2. Elution profiles for 15-μm latex particles at a flow-rate of 0.73 ml/min. Runs a and b are made in the conventional channel of uniform thickness with and without stopflow, respectively. Run c was also executed without stopflow, but in this case with pinched inlet channel system I.

specifically, the standard deviation σ_t in time units for the three profiles are 52, 141, and 46 s for Fig. 2a, b and c, respectively. The corresponding plate heights are 0.43, 3.7, and 0.52 mm, respectively.

We note that to fully utilize the capabilities of the pinched inlet channel system, the flow-rate must be matched to the dimensions of the pinched inlet segment in order to assure complete relaxation of all components before they enter the second stage, the separation segment. The flow-rate used in conjunction with Fig. 2 accordingly yields an h_0/L value of 0.26, well below the maximum allowable value of 0.4, equal to the ratio of the length of the pinched segment to the total channel length.

Figs. 3 and 4 further illustrate the need to match the operating flow-rate to the dimensions of the pinched (relaxation) segment and the consequences of failing to adhere to the required relationship. These figures show the elution profiles of the two particle diameters in systems I and II expressed along the elution volume axis. In "normal" (non-steric) FFF operation, the peaks observed at different flow-rates would be expected to center about the same mean elution volume position, differing only in peak width. The figures show that other factors are involved in the present study.

Fig. 3a shows the elution profiles of a 15-μm latex particle eluted from system I under different flow conditions. The different flow velocities lead to different values of the ratio h_0/L; values of the latter are shown in the figure. The peak furthest right, for which $h_0/L = 0.21$, has been eluted with the lowest flow-rate, 0.58 ml/min. The peaks are displaced to the left as the flow-rate increases in the sequence 1.12, 1.34, and 1.79 ml/min, respectively. The two peaks with the greatest displacement to the left are

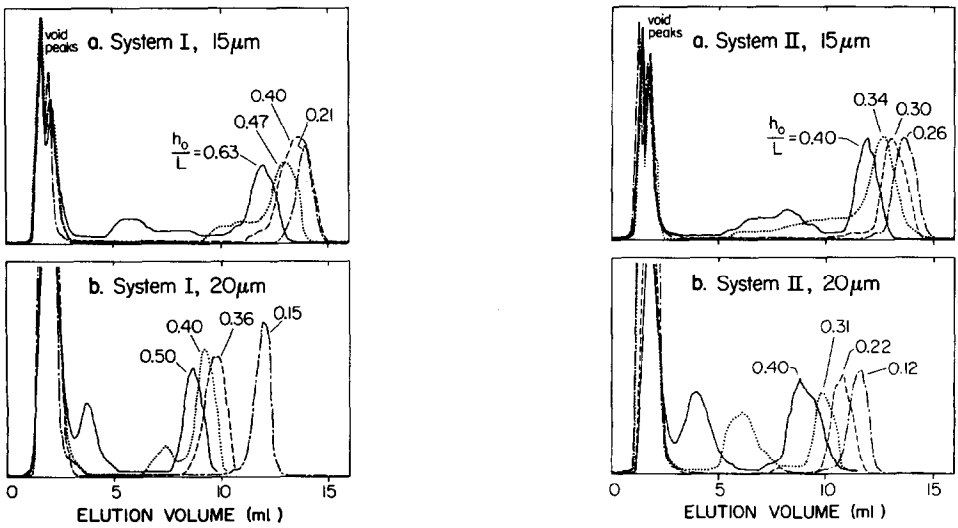

Fig. 3. Comparison of elution profiles at different flow-rates for 15-μm and 20-μm microspheres in pinched inlet system I. Values of the ratio h_0/L are shown. The flow-rates from left to right are 1.79, 1.34, 1.12, and 0.58 ml/min for panel a and 2.50, 1.98, 1.79, and 0.76 ml/min for panel b.

Fig. 4. Elution profiles of 15-μm and 20-μm latex particles at different flow-rates in system II. The flow-rates from left to right are 1.12, 0.94, 0.85, and 0.73 ml/min for panel a and 2.01, 1.55, 1.10, and 0.91 for panel b.

further distorted by satellite peaks or bumps preceding the main peak. These spurious peaks represent the early elution of a portion of the injected sample that has not been fully relaxed. Such distortions are expected when h_0/L exceeds the critical value 0.4. As seen in the figure, the critical h_0/L ratio is greater than 0.4 for both of the distorted peaks; in the worst case this ratio is 0.63 and the corresponding peak is associated with a prominent early satellite peak.

While the appearance of satellite peaks is associated with the failure to achieve complete relaxation, some other mechanism must be sought to explain the shift in the position of the main peak with changes in flow-rate. While not expected in the normal operating mode of FFF, such shifts are common in steric FFF[9] and reflect the increasing influence of lift forces with increasing flow-rate.

Fig. 3b, involving 20-μm particles in system I, shows much the same effect. In this case, too, the leading satellite peaks are associated with the larger h_0/L values. However, we note that a small satellite peak is still found when h_0/L reaches its threshold value of 0.40. This may be due to the fact that the actual relaxation of particles in a confined channel, particularly when they are very near the channel walls, is somewhat slower than that calculated from the Stokes equation which serves as the basis for eqn. 7. Thus relaxation times, particularly for larger particles, may be somewhat longer than calculated, giving h_0/L values somewhat greater than the ideally calculated values shown in the figure. In accordance with this hypothesis, the satellite peak has disappeared by the time h_0/L has dropped only slightly to 0.36.

Similar results are shown in Fig. 4 for system II, in which the relaxation segment is even thinner, 76 μm in place of 127 μm. While the same overall effects are apparent in the two figures, the satellite peaks have become more prominent in Fig. 4. Thus in Fig. 4a, a significant satellite bump is still present for the case in which h_0/L has dropped to 0.34, well below the threshold. Only when this ratio drops to 0.30 does the satellite profile become largely eliminated. This heightened departure from ideal relaxation in Fig. 4 is again consistent with the hypothesis that an anomaly arises due to the decreased transport rate and increased relaxation time expected for large particles in thin channels. Since the thickness of the relaxation segment has dropped from 127 to 76 μm in going from Fig. 3 to Fig. 4, the increasing departure from ideal relaxation is expected. This conclusion is further reinforced by Fig. 4b, showing runs with 20-μm instead of 15-μm particles. Here, a major satellite is still found with $h_0/L = 0.31$, but has disappeared by the time this ratio reaches 0.22.

In general, the departure from the ideally calculated h_0/L value will increase with the ratio of the particle diameter to the thickness of the relaxation segment. Fig. 4b has the largest ratio and, correspondingly, the largest departure. For particles of submicron size separated by the normal operating mode of FFF, the departure should be negligible for almost any practical thickness of the relaxation segment. We note that the anomaly unique to the relatively large particles subject to analysis by steric FFF can be neutralized by dropping to slightly lower flow-rates than those calculated on the basis of eqn. 9 subject to the condition $h_0 \leqslant L_1$.

We note that lift forces, as such, should not lead to anomalous satellite peaks. With strong lift forces, the particles will not settle to a position where they make contact with the accumulation wall. Instead, the particles will be pushed by lift forces away from the wall, where they will form a thin band or hyperlayer. Upon passage from the relaxation to the separation segment, the equilibrium hyperlayer position

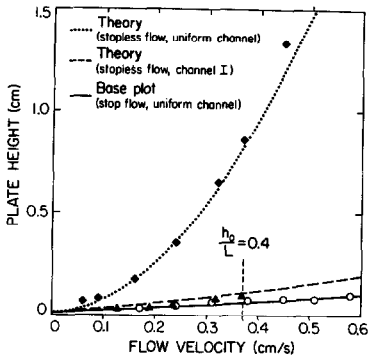

Fig. 5. Observed plate height *versus* mean flow velocity plots contrasting performance of pinched inlet channel I and uniform channel under stopless flow conditions. Experimental data: (◆) stopless flow, uniform channel; (▲) stopless flow, channel I; (○) stopflow, uniform channel.

may change significantly relative to the various streamplanes in the channel. However, as long as all particles emerge from the relaxation segment in a thin band, the transition should lead to little additional dispersion no matter what the relative positions of the bands in the two segments are. Thus, in general, the object of the relaxation segment is to rapidly gather component particles into a thin lamina whose position can lie anywhere between the channel walls.

The efficacy of the pinched inlet structure is further illustrated in the plate height *versus* velocity plots of Fig. 5, obtained for the 15-μm latex. The lower plot is based on measured values (open circles) of plate height ($\hat{H}$ based on eqn. 11) obtained for the uniform (non-pinched) channel structure under the stopflow conditions. The plot immediately above applies to pinched inlet channel I operated under stopless flow conditions. The experimental points (solid triangles) do not lie significantly higher than those of the lower plot, despite the stopless flow operation. The dashed line, calculated from eqn. 18 [where the lower plot is taken as the base plot corresponding to H_1 (stopflow)], verifies that there is little increase in the plate height when the pinched inlet configuration is used for stopless flow. However, stopless flow operation with the uniform channel displays a dramatic rise in plate height as illustrated by the experimental points (solid diamonds) and theoretical curve (dotted line) of the upper plot. These plots clearly illustrate the potential usefulness of the pinched inlet configuration for a stopless flow operation in FFF.

ACKNOWLEDGEMENT

This work was supported by Grant GM10851-33 from the National Institutes of Health.

REFERENCES

1 J. C. Giddings, *Sep. Sci. Technol.*, 24 (1989) 755.
2 F. J. Yang, M. N. Myers and J. C. Giddings, *Anal. Chem.*, 49 (1977) 659.
3 J. C. Giddings, *Anal. Chem.*, 57 (1985) 945.
4 M. E. Hovingh, G. H. Thompson and J. C. Giddings, *Anal. Chem.*, 42 (1970) 195.

5 R. E. Peterson II, M. N. Myers and J. C. Giddings, *Sep. Sci. Technol.*, 19 (1984) 307.
6 C. A. Price, *Centrifugation in Density Gradient*, Academic Press, New York, 1982.
7 J. C. Giddings, *Anal. Chem.*, 35 (1963) 353.
8 J. C. Giddings, M. N. Myers, K. D. Caldwell and S. R. Fisher, in D. Glick (Editor), *Methods of Biochemical Analysis*, Vol. 26, Wiley, New York, 1980, p. 79.
9 T. Koch and J. C. Giddings, *Anal. Chem.*, 58 (1986) 994.